JOURNAL OF PROPULSION AND POWER
Vol. 9, No. 3, May–June 1993

Numerical Simulation of Turbine "Hot Spot" Alleviation Using Film Cooling

Daniel J. Dorney* and Roger L. Davis†
United Technologies Research Center, East Hartford, Connecticut 06108

Experimental data have shown that combustor hot streaks can lead to pressure side "hot spots" on first-stage turbine rotor blades. In previous numerical studies, it has been shown that unsteady Navier-Stokes procedures can be used to predict the rotor pressure surface temperature increase associated with these combustor hot streaks. In the current investigation, similar two-and three-dimensional unsteady Navier-Strokes simulations have been performed to demonstrate the use of numerical tools in the optimization of film cooling configurations. In this study, the addition of prudently placed film cooling holes along the rotor pressure surface is shown to significantly diminish the adverse effects of the hot streak. Using a two-dimensional Navier-Stokes procedure, a parametric study was performed to determine the impact of the location of the film cooling holes, fluid injection velocity, and fluid injection angle on the time-averaged rotor surface temperature. The experience gained from these two-dimensional simulations was then applied to a series of three-dimensional simulations in which the effects of the film cooling hole distribution on the rotor pressure surface temperature were studied. The results of these simulations indicate that computational procedures can be used to design feasible film cooling schemes which eliminate the adverse effects of combustor hot streaks.

Nomenclature

a	=	speed of sound
e_t	=	total energy
L	=	reference length, 1.0 in./0.254 m
M	=	Mach number
P	=	static pressure
q	=	heat flux
Re	=	freestream inlet reference Reynolds number
r	=	radius
S	=	surface arc length
T	=	static temperature
u, v, w	=	x, y, z components of velocity
ρ	=	density
Ω	=	rotor rotational speed

Subscripts

fc	=	film cooling
hs	=	hot streak
ms	=	midspan
t	=	stagnation quantity
x, y, z	=	first derivative with respect to x, y, or z
1	=	inlet quantity
2	=	exit quantity

Introduction

EXPERIMENTAL data taken from gas turbine combustors indicate that the flow exiting the combustor can contain both circumferential and radial temperature gradients. These temperature gradients arise from the combination of the combustor core flow with the combustor bypass and combustor surface cooling flows. It has been shown both experimentally and numerically[1–4] that temperature gradients, in the absence of total pressure nonuniformities, do not alter the flow within the first-stage turbine stator, but do have significant impact on the secondary flow and wall temperature of the first-stage rotor. Combustor hot streaks, which can typically have temperatures twice the freestream stagnation temperature, increase the extent of the secondary flow in the first-stage rotor and significantly alter the rotor surface temperature distribution. A combustor hot streak such as this has a greater streamwise velocity than the surrounding fluid, and therefore, a larger positive incidence angle to the rotor as compared to the freestream. Due to this rotor incidence variation through the hot streak and the slow convection speed on the pressure side of the rotor, the hot streak accumulates on the rotor pressure surface creating a hot spot. It has been shown that thermal fatigue due to a combustor hot streak can significantly reduce the life of a turbine blade.[1]

In an effort to alleviate excessive turbine blade surface temperatures, design engineers often place film cooling holes along the airfoil surface. The cooling air, which is normally bled from the compressor, acts as a buffer between the blade surface and the hot gases contained in the mainstream flow. While film cooling of a turbine blade can reduce thermal stresses, interaction of the injected fluid with the mainstream flow can sometimes cause a degradation of the overall aerodynamic efficiency.[5] In addition, since the mass flow used for film cooling bypasses the combustor, excessive film cooling can result in unnecessary reduction of overall engine thrust. Therefore, the placement of the film cooling holes, the temperature and mass flow rate of the injected fluid, and the fluid injection angle are all crucial to the performance and durability of turbine blades, as well as overall engine performance.

The focus of the current effort has been to demonstrate the use of two- and three-dimensional viscous, unsteady rotor/stator interaction numerical simulations in determining feasible cooling schemes which alleviate the adverse effects of combustor hot streaks. This study also attempts to provide additional insight into the phenomenon of hot-streak migration. The present research does not concentrate on the details of the interaction between the film cooling and mainstream flows in the vicinity of the film cooling injection holes, but rather on the migration of the film cooling fluid downstream of the injection holes and the elimination of the high-temperature effects associated with hot streaks. In this investi-

Presented as Paper 92-3309 at the AIAA/SAE/ASME/ASEE 28th Joint Propulsion Conference, Nashville, TN, July 6–8, 1992; received July 13, 1992; revision received Nov. 9, 1992; accepted for publication Nov. 23, 1992.

*Associate Research Engineer, Computational and Design Methods Group. Member AIAA.

†Senior Principle Engineer, Computational and Design Methods Group. Member AIAA.

gation, two- and three-dimensional unsteady Navier-Stokes analyses are used to predict the effects of rotor film cooling and stator base cooling on surface heat transfer in the first stage of a turbine including the presence of a combustor hot streak. Using a two-dimensional unsteady Navier-Stokes procedure, a parametric study was performed on a 1-stator/1-rotor/1-hot-streak configuration to determine the impact of the location of the film cooling holes, fluid injection velocity, and fluid injection angle on the time-averaged rotor surface temperature. The experience gained from these two-dimensional simulations was then applied to a series of three-dimensional 1-stator/1-rotor/1-hot streak simulations, in which the effects of the film cooling hole distribution on the rotor pressure surface temperature were studied. The results from these computations have been compared to the experimental data reported by Butler et al.[1] and Roback and Dring.[2] The numerical results, and their comparison with the available experimental data, sheds new insight into the phenomena of hot-streak migration and the alleviation of rotor surface heating through the use of rotor film cooling and stator base cooling.

Numerical Integration Procedure

The governing equations considered in this study are the time-dependent, three-dimensional Reynolds-averaged Navier-Stokes equations

$$\boldsymbol{U}_t + \boldsymbol{F}_x + \boldsymbol{G}_y + \boldsymbol{H}_z = 0 \tag{1}$$

where the vector $\boldsymbol{U}$ represents the primary variables, ρ, ρu, ρv, ρw, and e_t. The vectors $\boldsymbol{F}$, $\boldsymbol{G}$, and $\boldsymbol{H}$ represent the components of the inviscid and viscous mass, momentum, and energy fluxes. The viscous fluxes are simplified by incorporating the thin-layer assumption.[6] In the current study, viscous terms are retained in the direction normal to the hub surface (z direction), and in the direction normal to the blade surface (y direction). To extend the equations of motion to turbulent flows, an eddy viscosity formulation is used and the turbulent viscosity is calculated using the Baldwin-Lomax[6] algebraic turbulence model. The effects of film and base cooling on the turbulence field were not modeled since the focus of the current investigation was not on the local details of the film cooling fluid, but on the elimination of the high-temperature effects associated with combustor hot streaks.

The numerical procedure for the three-dimensional analysis consists of a time-marching, implicit, third-order spatially accurate, upwind, finite-difference scheme. The inviscid fluxes are discretized according to the scheme developed by Roe.[7] The viscous fluxes are calculated using standard central differences. An alternating direction implicit technique is used to compute the time rate changes in the primary variables. In addition, Newton subiterations can be used at each global time step to increase stability and reduce linearization errors. For all cases investigated in this study, three Newton subiterations were performed at each time step. The numerical procedure used for the two-dimensional algorithm is similar to that used in the three-dimensional analysis, except that the inviscid fluxes are discretized according to the scheme developed by Osher.[8] Further details of the two- and three-dimensional numerical techniques can be found in Refs. 3, 9, and 10.

Boundary Conditions

The theory of characteristics is used to determine the boundary conditions at the inlet and exit of the computational domain. For subsonic inlet flow, the total pressure, v and w velocity components, and the downstream running Riemann invariant $R_1 = u + [2a/(\gamma - 1)]$ are specified, while the upstream running Riemann invariant $R_2 = u - [2a/(\gamma - 1)]$ is extrapolated from the interior of the computational domain. For simulations containing inlet hot streaks, the boundary conditions within the hot streak must be modified. Within the hot streak the inlet flow variables used to define the specified boundary conditions can be written as

$$\begin{aligned} u_{hs} &= u_\infty\sqrt{T_{hs}/T_\infty} \qquad v_{hs} = v_\infty\sqrt{T_{hs}/T_\infty} \\ w_{hs} &= w_\infty\sqrt{T_{hs}/T_\infty} \qquad P_{hs} = P_\infty \\ a_{hs} &= a_\infty\sqrt{T_{hs}/T_\infty} \qquad \rho_{hs} = \rho_\infty/(T_{hs}/T_\infty) \end{aligned} \tag{2}$$

where T_{hs} is the temperature within the hot streak, and T_∞ is the temperature of the undisturbed inlet flow. Similar to the experimental flow conditions,[1] the static and total pressure within the hot streak are set equal to that of the undisturbed inlet flow.

For subsonic outflow, the v and w velocity components, entropy, and the downstream running Riemann invariant are extrapolated from the interior of the computational domain. The pressure ratio, P_2/P_{t1}, is specified at midspan of the computational exit, and the pressure at all other radial locations at the exit is obtained by integrating the equation for radial equilibrium. A periodicity condition is enforced at midpassage in the circumferential (θ) direction.

For viscous simulations, no-slip boundary conditions are enforced at the hub and shroud endwalls of the blade passage and along the surface of the stator and rotor airfoils. It is assumed that the normal derivative of the pressure is zero at solid wall surfaces. In addition, a specified heat flux distribution is held constant in time along the solid surfaces. For film cooling applications, the viscous boundary conditions are modified at discrete points corresponding to the film cooling injection holes. In the current study, film cooling is being modeled using a surface transpiration boundary condition. The simulation of film cooling is accomplished by specifying

$$|V_{fc}|,\ \theta_1,\ \theta_2,\ T_{fc},\ \rho_{fc} \tag{3}$$

where $|V_{fc}|$ is the magnitude of the film cooling injection velocity, θ_1 and θ_2 are the specified injection angles with respect to the axial and spanwise directions (as measured from the local surface tangents), respectively, T_{fc} is the temperature of the film cooling fluid, and ρ_{fc} is the density of the film cooling fluid. The density of the film cooling fluid in this study is chosen such that the static pressure at an injection location is equal to the time-averaged static pressure obtained in the absence of film cooling.

The flow variables of U at zonal boundaries are explicitly updated after each time step by interpolating values from the adjacent grid. The zonal boundary conditions are nonconservative, but for subsonic flow this should not affect the accuracy of the final flow solution.

Grid Generation and Geometry

The three-dimensional Navier-Stokes analysis uses five zonal grids to discretize the rotor-stator flowfield and facilitate relative motion of the rotor. A combination of O- and H-grid sections are generated at constant radial spanwise locations in the blade-to-blade direction extending upstream of the stator leading edge to downstream of the rotor trailing edge. Algebraically generated H-grids are used in the regions upstream of the leading edge, downstream of the trailing edge, and in the interblade region. The O-grids, which are body-fitted to the surfaces of the airfoils and generated using an elliptic equation solution procedure, are used to properly resolve the viscous flow in the blade passages and to easily apply the algebraic turbulence model. Grid generation for the two-dimensional analysis is similar to that for the three-dimensional procedure, except that the O-grids are patched, rather than overlaid, into the H-grids.

Results

A series of numerical experiments simulating hot-streak migration through a turbine stage have been conducted using two- and three-dimensional unsteady Navier-Stokes procedures. The predicted results of the numerical simulations have been compared with the experimental data reported by Butler et al.[1] and Roback and Dring.[2]

The geometry used in the experimental tests was the first stage of the United Technologies Large Scale Rotating Rig (LSRR)[1,11] which includes 22 stator airfoils and 28 rotor airfoils. The LSRR is a large-scale, low-speed, rotating-rig windtunnel facility designed to simulate the flowfield in axial-flow turbomachines. For the hot streak experiments, the LSRR was configured to resemble the first stage of a high-pressure turbine, typical of those used in aircraft gas turbine designs.

In the first experimental study,[1] one hot streak was introduced through a 5.08-cm-diam circular pipe at 40% span, and midway between two stator airfoils of the LSRR. The temperature of the hot streak was twice that of the surrounding inlet flow, whereas the static and stagnation pressures were identical to the freestream. The hot streak was seeded with carbon dioxide (CO_2), and the path of the hot streak was determined by measuring CO_2 concentrations at various locations within the turbine stage. The flow conditions used in the first experiment are shown in Table 1. In the following sections, the first experimental test will be referred to as the "circular hot streak no. 1 (CHS1)" experiment.

A second experimental study[2] was conducted using the same configuration as in the CHS1 experiment, except that the temperature of the hot streak was only 1.2 times that of the surrounding inlet flow, and the flow coefficient was slightly increased (see Table 2). In the following sections, this experimental test will be referred to as the "circular hot streak no. 2 (CHS2)" experiment.

Two-Dimensional Simulations

A series of two-dimensional 1-stator/1-rotor/1-hot-streak simulations with rotor film cooling and a specified heat flux have been performed to study possible techniques for alleviating the adverse effects of combustor hot streaks on first-stage turbine rotors. In this investigation, the number and location of the film cooling holes, the fluid injection velocity, and the level of the surface heat flux were all varied to obtain both the qualitative and quantitative characteristics of different film cooling schemes. The flow conditions used in the film cooling simulations are representative of the circular hot streak experiment (CHS2) and are shown in Table 2. Local details of the film cooling effects have not been validated with experimental data. However, the goal of the current investigation has been to determine the feasibility of using numerical simulations to guide film cooling design.

The computational grid topology used in the two-dimensional film cooling simulations is similar to that used in previous adiabatic simulations.[4,9] The two-dimensional simulations required approximately six cycles at 3000 time steps per global cycle on a four-processor Alliant FX-80 to obtain a time-periodic solution. A global cycle corresponds to the rotor blade rotating through an angle of $2\pi/N$, where N is the number of stator blades (i.e., $N = 1$). Typical calculations required 0.00191 s/grid point/time step computation time.

In the first portion of the film cooling investigation, the impact of film cooling injection hole location on the time-averaged rotor surface temperature was studied. Since the current goal of film cooling is to alleviate the excessive temperatures and thermal gradients which are observed on the pressure surface of first-stage turbine rotor blades in the presence of hot streaks, a film cooling injection hole (consisting of two adjacent streamwise computational grid points) was located at approximately 27% of the axial chord on the pressure surface of the rotor airfoil. The fluid was injected at a velocity equal to 0.2 times that of the inlet freestream velocity and at an angle of 10 deg with respect to the local surface tangent. The temperature of the injected fluid was specified to be 520°R (compared to 530°R for the freestream, and 636°R within the hot streak) and the density ratio was chosen such that the static pressure at the injection location was equal to the time-averaged static pressure obtained in the absence of film cooling. It is important that the injected fluid does not initiate boundary-layer separation, thereby reducing the turbine efficiency. Inspection of the time-averaged velocity vectors in the vicinity of the film cooling injection hole indicated that the specified film cooling conditions do not cause boundary-layer separation in the time-averaged flowfield. A mild negative heat flux of ($\dot{q} = -0.2$), which corresponds to a surface temperature approximately 5°R below the freestream temperature, was also specified along the surface of the rotor for all the film cooling simulations. A simulation with the heat flux alone and no film cooling produced time-averaged rotor surface temperatures which were essentially identical to those obtained from the adiabatic calculation.[4]

The time-averaged, maximum, and minimum pressure coefficient distributions for the airfoil surfaces were compared with the experimental data of Dring et al.[11] in Refs. 4 and 9. Likewise, comparisons between the predicted and experimental values of the unsteady pressure amplitude coefficient for the stator and rotor surfaces are given in Refs. 4 and 9. The predicted time-averaged and unsteady pressure coefficients show very good agreement with the experimental data.

Figure 1 illustrates the time-averaged rotor surface temperature coefficient distribution for the current simulation,

Table 1 Flow conditions for the CHS1 experiment

Flow coefficient, ϕ	0.68
Inlet Mach number, M_1	0.07
Rotor rotation speed, Ω	470 rpm
Reynolds number, Re	3.937×10^6/m
Axial gap, g	65%
Freestream temperature, T_1	530°R
Hot-streak temperature, T_{hs}	1060°R

Table 2 Flow conditions for the CHS2 experiments

Flow coefficient, ϕ	0.78
Inlet Mach number, M_1	0.07
Rotor rotation speed, Ω	410 rpm
Reynolds number, Re	3.937×10^6/m
Axial gap, g	65%
Freestream temperature, T_1	530°R
Hot-streak temperature, T_{hs}	636°R

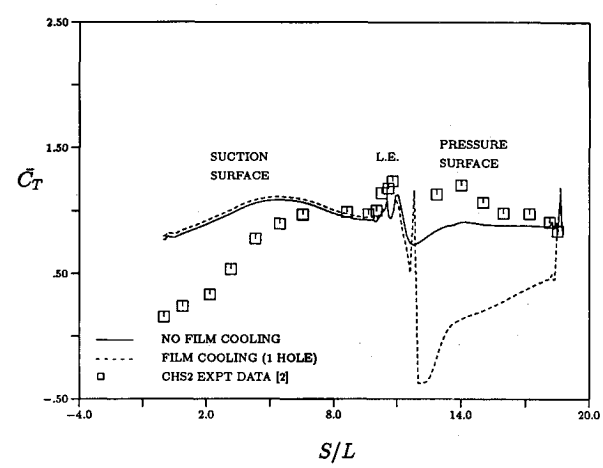

Fig. 1 Rotor temperature coefficient distributions for film cooling simulation—one hole.

where the temperature coefficient definition is defined as[3,4,9]

$$\bar{C}_T = \frac{T - T_1}{T_{\text{avgrle}} - T_1} \approx \frac{CO_2 - CO_{2\text{amb}}}{CO_{2\text{avgrle}} - CO_{2\text{amb}}} \quad (4)$$

where T is the local time-averaged temperature, T_{avgrle} is the midspan time-averaged temperature at the rotor leading edge, CO_2 is the experimentally obtained local time-averaged carbon dioxide concentration, and $CO_{2\text{avgrle}}$ is the experimental midspan time-averaged carbon dioxide concentration at the rotor leading edge. Equation (4) is similar to the definition of the film cooling *effectiveness* parameter, which is obtained if the time-averaged temperature at the rotor leading edge (T_{avgrle}) in Eq. (4) is replaced by the film cooling temperature. Included in Fig. 1 is the temperature coefficient distribution for the two-dimensional 1-stator/1-rotor hot-streak simulation without film cooling, and the CHS2 experimental data.[2]

The predicted results without film cooling are identical to those obtained in previous numerical simulations.[4] The predicted results without film cooling demonstrate fair agreement with the experimental data. The sources of the discrepancies between the predicted numerical results and the experimental data have been explained in detail in Refs. 4 and 9. With the addition of film cooling, a substantial reduction of the time-averaged temperature on the rotor pressure surface is observed in the vicinity of the film cooling hole. As the cooling fluid is convected downstream and away from the airfoil surface, the time-averaged surface temperature increases due to the influence of the hot streak. The time-averaged temperature on the suction surface of the rotor is basically unaffected by the pressure surface film cooling.

In an effort to further reduce the time-averaged temperature along the rotor pressure surface, a second film cooling hole (again modeled with two computational grid points) was added at approximately 47% axial chord on the pressure surface. Figure 2 shows the time-averaged temperature coefficient distributions from the simulation without film cooling, with one injection hole, and with two injection holes. The insertion of the second injection hole further reduces the time-averaged temperature along the aft portion of the rotor pressure surface, and again has little affect on the suction surface. The slope of the temperature gradient downstream of the second film cooling injection hole in Fig. 2 appears to be similar to the temperature gradient downstream of the first injection hole, suggesting that for the current injection conditions a linear relationship exists between the number of film cooling holes and the reduction of the time-averaged temperature. While the specified film cooling conditions have the desired effect of reducing the time-averaged temperature on the rotor pressure surface, they also create a numerically induced time-averaged temperature spike immediately upstream of the first injection hole. This spike is due to the sudden change from a no-slip to a transpiration boundary condition. Since the computational grids were not designed to resolve the local characteristics of the film cooling flow, the sudden change in the velocity at the injection holes resulted in the overprediction or underprediction of the density and pressure at the first grid point upstream of the injection hole.

The impact of the rotor surface film cooling injection velocity was also investigated. Two film cooling injection holes, located at 27 and 47% axial chord on the rotor pressure surface (each modeled with two adjacent streamwise computational grid points), were used in this portion of the study. The film cooling fluid temperature and injection angle were 520°R and 10 deg with respect to the local surface tangent, respectively. The injection velocities used were 0.05, 0.10, 0.20, and 0.40 of the inlet freestream velocity.

Figure 3 illustrates the rotor surface time-averaged temperature coefficient distributions for these simulations, along with the temperature distribution for the case without film cooling. Increasing the film cooling injection velocity is seen to increase the effectiveness of the film cooling, eventually ($V/V_\infty \approx 0.40$) eliminating the effects of the hot streak completely. Increasing the injection velocity also reduces the thermal gradients between adjacent film cooling holes, which is very important to structural designers. While increasing the injection velocity is beneficial in terms of reducing the time-averaged temperature, in reality, there are practical limits on the mass flow rate of the injected fluid, since the film cooling air is usually bled from the compressor.

A different approach used by turbomachinery designers to reduce the time-averaged temperature along the pressure surface of the rotor is to inject cooling fluid through the trailing edge (base) of the upstream stator airfoil. In the current study, cooling air was injected through a slot in the stator trailing edge (consisting of three computational grid points) in the direction of the mainstream flow. The temperature of the cooling fluid was specified to 424°R, and the density was chosen to yield a static pressure equal to that of the time-averaged solution without film cooling. The temperature of the cooling fluid was specified to be 20% less than the freestream temperature because the maximum temperature of the hot streak was specified to be 20% greater than the freestream temperature. The cooling fluid was injected with velocities equal to 0.50, 1.00, and 1.50 times that of the inlet freestream velocity.

Figure 4 illustrates the rotor surface time-averaged temperature coefficient distributions for these simulations, along with the temperature distribution for the case without film cooling. For the specified conditions, the use of stator base cooling has much less of an impact on the rotor surface tem-

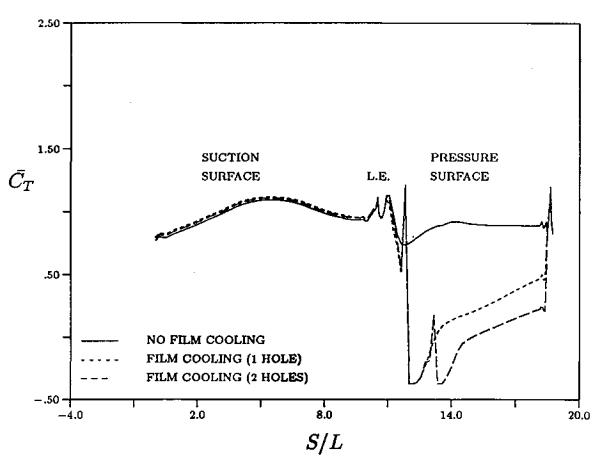

Fig. 2 Rotor temperature coefficient distributions for film cooling simulations—one and two holes.

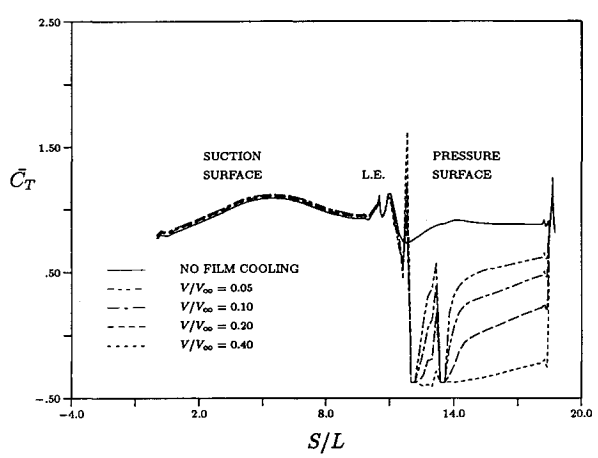

Fig. 3 Rotor temperature coefficient distributions for film cooling simulations with different injection velocities.

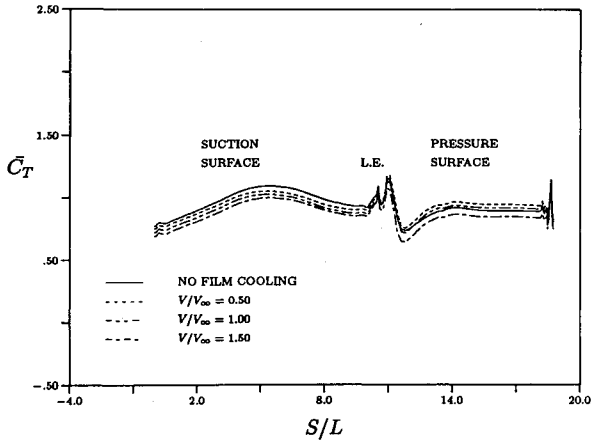

Fig. 4 Rotor temperature coefficient distributions for stator base cooling simulations.

Fig. 5 Static temperature contours for stator base cooling simulations.

peratures than film cooling the rotor airfoil. For all three injection velocities the time-averaged temperature on the suction surface of the rotor is reduced, the amount of the temperature reduction increasing linearly with the injection velocity. On the rotor pressure surface, however, the time-averaged temperature increases for the injection velocity less than freestream, stays approximately constant for the injection velocity equal to the freestream, and decreases for the injection velocity greater than the freestream. This is consistent with the experimental findings of Roback and Dring.[2] The base cooling fluid has a natural tendency to migrate towards the suction surface of the rotor for injection velocities at or below the local freestream velocity, whereas the hot streak has a tendency to migrate towards the pressure surface of the rotor (see Fig. 5, which is for a similar 3-stator/4-rotor calculation). Thus, when using stator base cooling to reduce the temperature of the rotor pressure surface, the current numerical simulations indicate that the injection velocity should be greater than the freestream velocity.

Three-Dimensional Simulations

A series of three-dimensional 1-stator/1-rotor/1-hot-streak simulations with a hot-streak temperature 20% greater than the freestream temperature, including rotor surface film cooling and a specified heat flux, have been performed to establish the effects of combustor hot streak migration on the time-averaged rotor surface temperature distribution. In these numerical simulations, one hot streak was introduced though a 5.08-cm-circular region at the inlet of each stator passage, corresponding to the 5.08-cm-diam pipe used in the CHS1 and CHS2 experiments.[1,2] The center of the hot streak was located at the midgap, 40% span location. A 15% axial gap was used between the rotor and stator airfoils. The inlet Mach number and rotor rotational speed are given in Table 1. The flow coefficient in the numerical simulations was $\phi = u/(r\Omega)_{ms} = 0.78$, and a midspan pressure ratio of $P_2/P_{t1} = 0.9630$ was determined from the inlet total pressure and the static pressure measured in the rotor trailing-edge plane. Further details regarding the operating conditions can be found in Refs. 4 and 9.

The grid system used in the three-dimensional simulations is identical to that used in Refs. 4 and 9, and is shown in Fig. 6. The three-dimensional calculations were performed on the NAS Cray 2 and Cray YMP supercomputers. Seven cycles at 2000 time steps per cycle were needed to obtain a time-periodic solution for the baseline adiabatic calculation,[4] while three additional cycles were needed for each of the simulations in the current study. These calculations required approximately 0.000263 s/grid point/time step computation time on the Cray 2.

In the first three-dimensional film cooling simulation, cooling fluid was injected through holes in the rotor pressure surface at a velocity equal to 0.2 times that of the freestream velocity, and at an angle of 25 deg, with respect to the local axial direction surface tangent. The film cooling injection angle was set at 25 deg (compared to 10 deg for the two-dimensional simulations) based on recent experimental investigations for the same geometry.[2] The temperature of the injected fluid was specified to be 520°R (2% lower than the freestream, and 22% lower than the hot streak) and the density ratio was chosen such that the static pressures at the injection locations were equal to the time-averaged static pressures in the absence of film cooling. The injection holes were located at 20 and 40% of the axial chord and extended from 20 to 80% of the span, at approximately 5% spanwise intervals. The total injected mass flow was equal to approximately 0.60% of the freestream mass flow. Similar to the two-dimensional simulations, two-adjacent grid points in the axial direction were used to model an injection hole. A total of 22 injection holes were used in the first stimulation. Inspection of the time-averaged velocity vectors in the vicinity of a film cooling injection hole near midspan indicated that the spec-

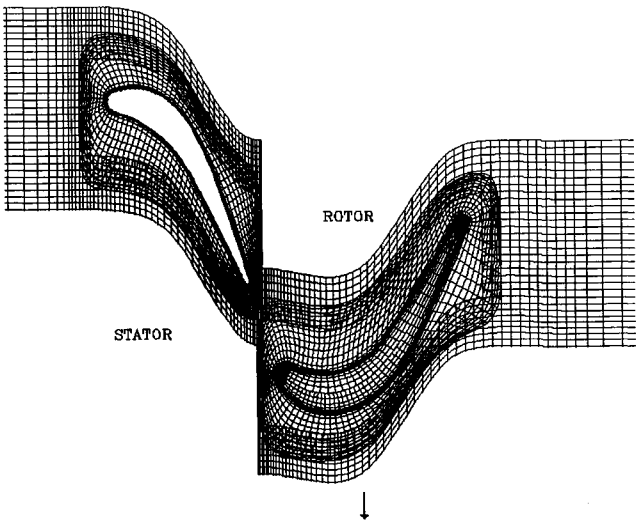

Fig. 6 Computational grid system.

ified film cooling conditions do not initiate boundary-layer separation in the time-averaged flowfield. A surface heat flux was also specified, which was designed to yield a surface temperature approximately 5 deg less than the local adiabatic surface temperature. Similar to the two-dimensional investigations, a three-dimensional simulation with only the specified heat flux, and no film cooling, produced rotor time-average temperatures nearly identical to those obtained in previous adiabatic simulations.[4] The predicted time-averaged and unsteady pressure distributions for this case are also essentially the same as those reported in Refs. 4 and 9.

Figure 7 illustrates the rotor surface midspan time-averaged temperature coefficient distributions for the simulation with only a surface heat flux, and the simulation with two film cooling rows and a surface heat flux. Also included in Fig. 7 are the CHS1 and CHS2 experimental data.[1,2] The differences between the experimental data and the predicted results (without film cooling) on the pressure surface of the rotor are related to the number of hot streaks present in the experiments and in the numerical simulations. In the experiments there was one hot streak introduced at the inlet to the turbine, while in the numerical simulations there were 22 hot streaks introduced at the inlet, i.e, one per stator passage.[9] The results for the simulation including film cooling show a substantial reduction of the midspan time-averaged temperature on the rotor pressure surface in the vicinity of the film cooling injection holes. As the cooling fluid convects downstream and away from the airfoil surface, the time-averaged surface temperature increases due to the influence of the hot streak. The time-averaged temperature on the rotor suction surface is unaffected, since the film cooling holes were placed only on the pressure surface.

In this three-dimensional simulation, the time-averaged surface temperature in the region between film cooling injection holes, and downstream of the last film cooling hole, increases much more rapidly than in the two-dimensional simulations. In spite of placing film cooling injection holes at 20 and 40% axial chord locations, the rapid mixing between the cooling fluid and the hot streak causes an increase in the temperature of the pressure surface near the trailing-edge region. This may be partially due to the interaction between the secondary and wall layer flows in the rotor passage, which cause the cooler injected fluid to mix very rapidly with the hot-streak fluid. This also explains why the rotor surface temperatures from the three-dimensional adiabatic simulation are much greater than those predicted in the two-dimensional adiabatic simulation.[4] Another cause of the temperature increase may be that the current injection angle (25 deg) is greater than that used in the two-dimensional simulations (10 deg). While it appears to be beneficial to reduce the injection angle, structural and manufacturing considerations limit the actual range of possible injection angles. The current injection

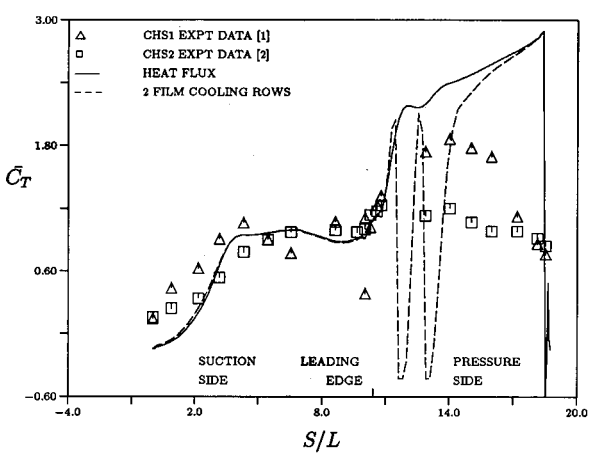

Fig. 7 Rotor midspan time-averaged temperature distribution—two rows film cooling.

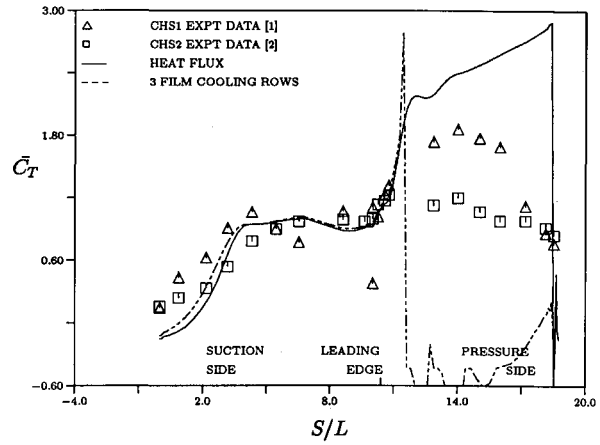

Fig. 8 Rotor midspan time-averaged temperature distribution—three rows film cooling.

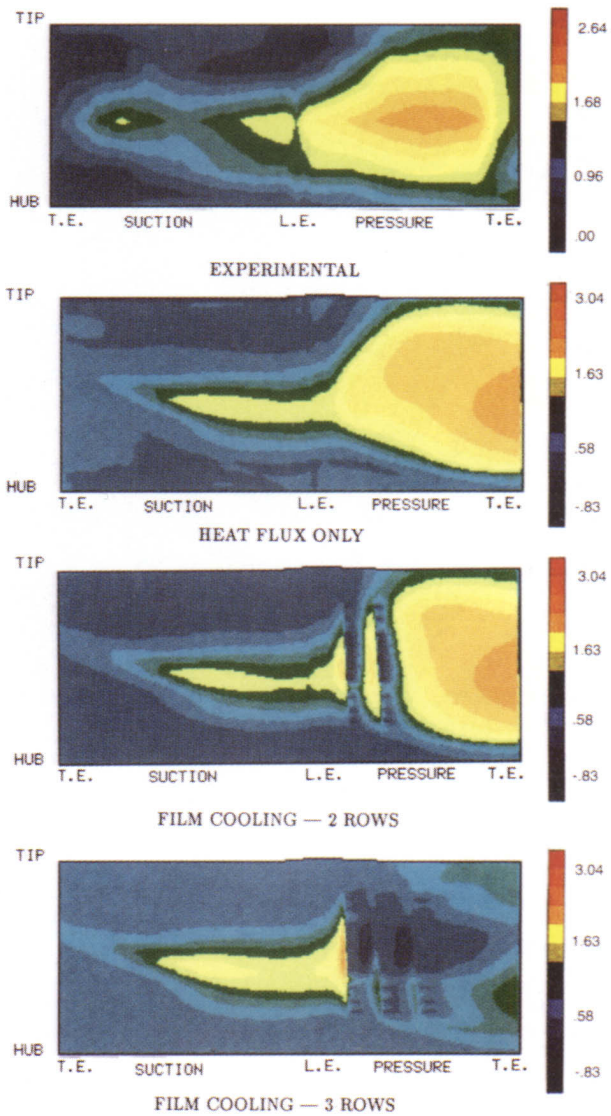

Fig. 9 Time-averaged surface temperature contours for LSRR rotor.

angle was chosen to be commensurate with those found in advanced gas turbines.

In an effort to eliminate the high time-averaged temperatures aft of midchord, a third row of film cooling holes was added at approximately 60% axial chord. Thus, in this simulation, a total of 33 film cooling holes (each consisting of two adjacent grid points) were used. In addition, the injection velocity was increased to 0.4 times that of the freestream

velocity. The total injected mass flow was equal to approximately 1.0% of the freestream mass flow. The heat flux was held at the same value as in the previous three-dimensional film cooling simulation. As before, the specified film cooling conditions do not cause boundary-layer separation in the time-averaged flowfield.

Figure 8 illustrates the rotor surface midspan time-averaged temperature coefficient distributions for the simulation with only a surface heat flux, and the simulation with three film cooling rows and a surface heat flux. As shown in this figure, the combination of a greater injection velocity and a third row of film cooling injection holes has eliminated most of the high-temperature regions on the rotor pressure surface. The high-temperature region aft of midchord has been reduced, as have the high-temperature regions between the film cooling injection holes. A time-averaged temperature spike, similar to that observed in the two-dimensional simulations, is located just upstream of the first row of film cooling holes for these film cooling conditions.

Figure 9 shows the experimental CO_2 contours for the CHS1 flow conditions, the predicted time-averaged temperature contours for the rotor surface with a specified heat flux only, with two rows of film cooling holes, and with three rows of film cooling holes. The film cooling locations are characterized by the dark blue (low temperature) contours. While discrete film cooling jets can be seen inboard of approximately 35% span and outboard of about 65% span, the cooling fluid near midspan appears to be contained with one continuous jet. As noted above, the film cooling injection holes were located at approximately 5% span increments. In the midspan region, the computational grid lines were also spaced approximately 5% of the span apart, resulting in six film cooling holes being placed at six consecutive grid points in the spanwise direction. Investigation of Fig. 9 reveals that increasing the injection velocity extends the range of effectiveness of the cooling fluid. This figure also illustrates that the addition of a third row of film cooling holes has significantly decreased the time-averaged rotor pressure surface temperature aft of the midchord point.

Figure 10 illustrates the predicted time-averaged temperature contours at a fixed axial station 10% of the axial chord downstream of the rotor trailing edge. The predicted contour levels were similar with and without rotor surface film cooling, as the cooling air only effects the local surface flow conditions. The corresponding experimental CO_2 concentration contours are also illustrated in Fig. 10. Both the predicted and experimental results indicate an elliptically shaped high-temperature region. This is consistent with the results of a previous numerical simulation,[4,9] which demonstrated that the hot streak is broken up into discrete temperature eddies as it migrates through the turbine passage. The hot fluid contained within the hot streak is "stretched" from the pressure side to the suction side of the passage by the difference in convection speeds, causing the apparent elongation of the contours.

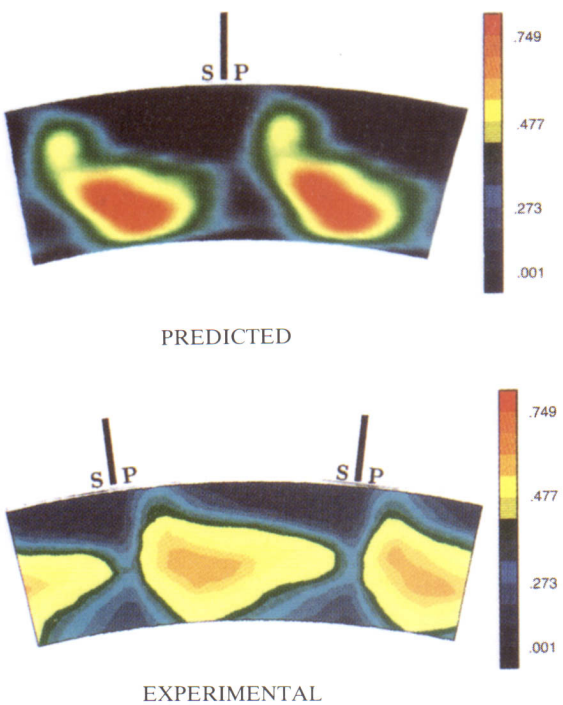

Fig. 10 Time-averaged temperature contours—10% downstream of trailing edge.

Conclusions

Experimental studies have shown that combustor hot streaks can significantly affect the secondary flows and wall temperatures of the first-stage turbine rotor. To gain insight into the interactions between hot streaks, secondary flows, and film cooling flows and their effects on the surface temperature distribution of a first-stage rotor, numerical simulations of hot streak migration through a turbine stage have been performed. The main goal of the current simulations has been to demonstrate the feasibility of using numerical simulations to guide the design of film cooling schemes.

Numerical simulations have shown that the addition of prudently located film cooling holes on the rotor pressure surface is a highly effective means of eliminating the adverse temperature effects of a hot streak on the rotor pressure surface. The cooling hole location, fluid injection angle, and fluid injection velocity were all varied to determine a reasonable and practical film cooling scheme. The results of this study indicate that two-and three-dimensional computational procedures can be used to develop feasible film cooling schemes. Injecting the cooling fluid through the base of the upstream stator was found to be less effective at cooling the rotor pressure surface, and is highly dependent on the fluid injection velocity. In particular, it was determined that the velocity of the fluid injected through the base of the stator must be greater than the freestream velocity to be useful for cooling the pressure surface of the rotor. Future research will focus on comparing numerical results with experimental data sets for film cooling and improving the turbulence model in the vicinity of film cooling holes.

Acknowledgments

This work was supported by the Naval Air Systems Command under NAVAIR Contract N00014-88-0677 from the office of George Derderian and Lewis Sloter, with Raymond Shreeve of the Naval Post Graduate School acting as technical monitor. This work was also supported by the United Technologies Research Center under the Corporate Research Program. The authors would like to thank Man Mohan Rai and Nateri Madavan of the NASA Ames Research Center for assistance in computational aspects of this investigation. The authors appreciate the helpful discussions with Robert Dring and Richard Roback of the United Technologies Research Center and Om Sharma of Pratt & Whitney concerning interpretation of the experimental and numerical results.

References

[1]Butler, T. L., Sharma, O. P., Joslyn, H. D., and Dring, R. P., "Redistribution of an Inlet Temperature Distortion in an Axial Flow Turbine Stage," *Journal of Propulsion and Power*, Vol. 5, No. 1, 1989, pp. 64–71.

[2]Roback, R. J., and Dring, R. P., "Hot Streaks and Phantom Cooling in a Turbine Rotor Passage: Part 1—Separate Effects," American Society of Mechanical Engineers Paper 92-GT-75, June 1992.

[3]Rai, M. M., and Dring, R. P., "Navier-Stokes Analyses of the Redistribution of Inlet Temperature Distortions in a Turbine," *Jour-*

nal of Propulsion and Power, Vol. 6, No. 3, 1990, pp. 276–282.

[4]Dorney, D. J., Davis, R. L., Edwards, D. E., and Madavan, N. K., "Unsteady Analysis of Hot Streak Migration in a Turbine Stage," *Journal of Propulsion and Power*, Vol. 8, No. 2, 1992, pp. 520–529.

[5]Yamamoto, A., Kondo, Y., and Murao, R., "Cooling-Air Injection into Secondary Flow and Loss Fields Within a Linear Turbine Cascade," American Society of Mechanical Engineers Paper 90-GT-141.

[6]Baldwin, B. S., and Lomax, H., "Thin-Layer Approximation and Algebraic Model for Separated Turbulent Flows," AIAA Paper 78-257, Jan. 1978.

[7]Roe, P. L., "Approximate Riemann Solvers, Parameter Vectors, and Difference Schemes," *Journal of Computational Physics*, Vol. 43, No. 2, 1981, pp. 357–372.

[8]Chakravarthy, S., and Osher, S., "Numerical Experiments with the Osher Upwind Scheme for the Euler Equations," AIAA Paper 82-0975, June 1982.

[9]Dorney, D. J., Davis, R. L., and Edwards, D. E., "Investigation of Hot Streak Migration and Film Cooling Effects on Heat Transfer in Rotor/Stator Interacting Flows, Final Report," NAVAIR, N000140-88-C-0677, April 1992.

[10]Rai, M. M., "Three-Dimensional Navier-Stokes Simulations of Turbine Rotor-Stator Interaction," *Journal of Propulsion and Power*, Vol. 5, No. 3, 1989, pp. 307–319.

[11]Dring, R. P., Joslyn, H. D., Hardin, L. W., and Wagner, J. H., "Turbine Rotor-Stator Interaction," *Journal of Engineering for Power*, Vol. 104, Oct. 1982, pp. 729–742.